HIGH ENERGY ELECTRON SPIKES AT HIGH LATITUDES

J. W. Brown and E. C. Stone

California Institute of Technology
Pasadena, California 91109

CALIFORNIA INSTITUTE OF TECHNOLOGY

PASADENA, CALIFORNIA

HIGH ENERGY ELECTRON SPIKES AT HIGH LATITUDES

J. W. Brown and E. C. Stone

California Institute of Technology
Pasadena, California 91109

January 1972

SRL 72-1

HIGH ENERGY ELECTRON SPIKES AT HIGH LATITUDES

J. W. Brown and E. C. Stone*

California Institute of Technology
Pasadena, California 91109

ABSTRACT

Over 750 spikes of precipitating electrons with $E \geq 425$ kev were observed aboard the low altitude polar orbiter OGO 4 between 30 July 1967 and 31 December 1967. The spikes may be divided into three distinct populations depending on whether they occur at latitudes below, at, or above the local limit of trapping. These are designated type 1, 2, and 3, respectively. Type 3 spikes occur in a narrow latitude band about 3° wide, centered at Invariant Latitude $\Lambda \approx 78°$ at 1000 MLT (Magnetic Local Time) and 68° at 2000 MLT. Their relative frequency of occurrence, intensity, and hardness do not depend significantly on MLT. They appear to be associated with spikes observed near the magnetopause and neutral sheet. Type 2 spikes also occur in a latitude band about 3° wide, centered at about 71° at 1000 MLT and 67° at 2200 MLT. Their frequency of occurrence is highly dependent on MLT, with a large maximum near 2300, and very few events between 0600 and 1200. They appear to be related to island fluxes in the neutral sheet, although they occur on closed field lines and may persist for many hours. Type 1 spikes occur in a wider band of latitudes,

* Alfred P. Sloan Research Fellow

from about 62° to 68° near midnight, and 66° to 68° near noon. The local time dependence of their frequency of occurrence is similar to that of type 2 spikes, but less pronounced. Although they are observed on closed field lines, they do not persist for periods longer than about one hour, and we conclude that they are produced by strong pitch-angle scattering from the stably trapped population. The average spectral index (assuming a power-law spectrum) is 3 to 5, and the median flux (> 425 kev) is about 150 electrons $cm^{-2}sec^{-1}ster^{-1}$, although type 2 events near midnight tend to be larger and harder. All types tend to be more intense and to occur at lower latitudes when Kp is large.

Introduction

We will discuss phenomena known as "electron spikes" or "particle spikes". These are defined as brief, rapid increases in counting rate as observed by a particle detector, in this case aboard a low altitude, polar orbiting spacecraft. Numerous experimenters have observed "spikes" of electrons at high latitudes, ranging in energy from 0.7 kev [Hoffman and Evans, 1968; Hoffman, 1969] to above 500 kev [Anderson et al., 1968; McCoy, 1969]. In addition, electron "islands" having similar characteristics have been reported in the geomagnetic tail [Montgomery et al., 1965; Anderson, 1965; Murayama and Simpson, 1968; Retzler and Simpson, 1969], in the vicinity of the bow shock [Frank and Van Allen, 1964; Anderson et al., 1965], and near the equatorial plane at moderate distances (5-10 R_E) [Frank, 1965; Rosen, 1965; Arnoldy and Chan, 1969]. It is difficult to make definite

connections between these various events because of the small probability of having several spacecraft properly positioned and aligned at the time an event occurs. One such identification has apparently been made by Hones et al. [1971], who observed a spike simultaneously at 1, 6.6 and 18 R_E.

Spike observations at low altitudes by polar orbiting spacecraft offer the advantage of frequent sampling of field lines where spikes are usually seen. This makes possible statistical studies of the distribution and behavior of these events, which are necessary to determine their effect on the energy budget and particle populations within the magnetosphere and their relationships to other processes. The purpose of this paper is to present such a statistical study in which the effects of relevant physical parameters are represented with sufficient accuracy to be a useful basis for further theoretical calculations.

It should be emphasized that the present results represent events with electron energies $E_e \geq 425$ kev. There seems to be very little correlation between spikes in this energy range and those observed by Hoffman and Evans [1968] in the energy range 0.7 kev $\leq E_e \leq$ 24 kev. Likewise, the phenomena observed here differ significantly from those reported by McDiarmid and Burrows [1965] for $E_e \geq 40$ kev. However, at least part of our observations may be related to those of Fritz and Gurnett [1965] for $E_e \geq 10$ kev. We will examine the relationships between these observations, especially with respect to various possible source mechanisms.

Description of Experiment

The OGO 4 spacecraft was launched into a low altitude polar orbit on 28 July 1967. Initial orbit parameters were: apogee 908 km, perigee

412 km, inclination 86°, period 98 minutes. The spacecraft was oriented so that the University of Chicago/California Institute of Technology vertical particle telescope (Experiment D-08) faced radially away from Earth. The experiment also included a horizontal detector which was insensitive to electrons and which will not be discussed here.

A cross section of the vertical telescope is shown in Figure 1. The detector system is described in detail by Evans et al. [1970]. The opening half-angle of 30°, combined with the radial orientation of the symmetry axis, ensures that the telescope is responding primarily to precipitating particles at Invariant Latitudes $\Lambda \gtrsim 45°$. Mirroring particles will be detected at these latitudes only if they scatter from the telescope wall.

Table 1 indicates the response of the telescope to various particle types. The upper cutoff energies in each case are set by the anticoincidence scintillator D3. The rates indicated in Table 1 are monitored, and the particle energy loss in D1 is pulse-height analyzed for each event satisfying the $D1\overline{D3}$ requirement. A flag is set for each analyzed event indicating whether or not D2 was triggered in coincidence with D1. Because of the electronic thresholds of the detectors (425 kev for D1 and 250 kev for D2), electrons which leave enough energy in D1 to be detected cannot reach D2, and electrons which leave enough energy in D2 to be detected will not have left enough in D1. Therefore there is a very low probability that electrons cause any D1D2 true coincidences, and we know we are observing mostly electrons whenever the $D2\overline{D3}$ rate is large compared to the $D1D2\overline{D3}$ rate. Pulse-height data have been used in several instances to confirm the above conclusions.

The basic data used in the present work are plots of: D3 rate (averaged over 1.44 sec intervals), $D1\overline{D3}$ rate, $D2\overline{D3}$ rate, and $D1D2\overline{D3}$ rate (the last three quantities averaged over approximately 15 second intervals). These data and descriptive text [Evans et al., 1970] will be submitted to the National Space Science Data Center.

Spectral Response

A simulation of the detector system was exposed to electrons from a β source. Monoenergetic electrons were selected by means of a magnetic spectrometer. The true flux of particles at each energy was measured using a thick total-E detector. The outputs of the telescope detectors were pulse-height analyzed, and the detection efficiency determined as a function of discriminator threshold. The detection efficiency for discriminator thresholds of 425 kev for D1 and 250 kev for D2, multiplied by the geometrical factors for $D1\overline{D3}$ and $D2\overline{D3}$, give effective geometrical factors as functions of energy [Lupton and Stone, 1972]. We determined that approximately half of the $D1\overline{D3}$ response to an isotropic flux is due to electrons scattered from the magnesium wall of the telescope, but that only about 20% of the $D2\overline{D3}$ response arises from this source.

These functions were approximated by piecewise power-law fits over various energy intervals, and folded with various assumed power-law energy spectra to obtain expected counting rates in each detector as functions of the incident electron spectrum. The same process was carried out for various assumed exponential spectra using exponential fits to the effective geometrical factors. Using these computations, it is possible to obtain a limited amount of spectral information from the ratio $D1\overline{D3}/D2\overline{D3}$.

Preliminary calculations using the results of Fan et al. [1966] indicated that pileup in D1 might be important for some of the largest spikes encountered. The pulse pileup effect is important only in the case of electrons in D1, where the threshold is set electronically. The D2 threshold is set primarily by the requirement that the particle have sufficient range to penetrate D1 and the aluminum absorber, and still leave 250 kev in D2. Thus the $D2\overline{D3}$ counting rate cannot be due to the pileup of lower energy ($\lesssim$ 600 kev) electrons. In order to estimate the size of the pileup effect, we performed Monte Carlo calculations of the response of D1 to various input fluxes. The result of the calculation was, as one would expect, that the $D1\overline{D3}$ count rate includes a significant contribution from pileup effects when that rate is larger than $\sim$ 100 sec^{-1}. Since D2 is unaffected by pileup, the $D2\overline{D3}$ count rate (corrected for dead time) can be relied upon at all reasonable count rates.

Description and Classification of Spikes

Particle "spikes" are generally defined by their appearance as narrow peaks in plots of counting rate versus time (or some other parameter such as Invariant Latitude which varies smoothly with time). It is impossible to determine, when looking at an individual spike, whether the rapid variation is a spatial or temporal phenomenon. Observed on a low-altitude polar orbiting spacecraft, they generally have "widths" of a few seconds, corresponding to a few tenths of a degree in latitude. High time-resolution ion chamber data [McCoy, 1969; M. J. George, personal

communication, 1970] indicate typical widths of 0.25° to 2° in Invariant Latitude, or about 5 to 40 seconds in UT. Thus, our averaging time of 15 seconds in the count-rate plots may obscure some of the smaller, narrower spikes. For this reason, the D3 rate plot (with shorter averaging time) occasionally shows spikes which are not visible in the $D1\overline{D3}$ or $D2\overline{D3}$ rates.

We have observed a few spikes for which higher data rates were available. Because of the factor of 8 increase in bit rate, pulse-height data from these events could be examined with reasonable counting statistics using 2-second time resolution. Four events thus examined had widths (FWHM) of about 6, 8, 10, and 40 seconds, as indicated by the electron channels of the D1 pulse-height analyzer. (Due to the large statistical fluctuations in the electron energy loss process, pulse-height data from this experiment yields only minimal spectral information for electrons. However, pulse-height information does provide positive identification of electrons.) Figure 2 shows two of these events. Notice that the D3 rate does not track exactly with the $D1\overline{D3}$ rate, probably because D1 and D3 have different energy and angular response characteristics.

Disagreement between McDiarmid and Burrows [1965] and McCoy [1969] about the Λ - MLT occurrence of spikes and the observation by McCoy [1969] that the local time dependence for spikes occurring above the trapping boundary is different from that for those below, suggest that there may be several distinct populations of spikes, and that each should be examined separately. We divided the spikes we observed into three types, according to whether they occur below, at, or above the outer zone boundary determined for each pass. These will be referred to

as type 1, type 2, and type 3, respectively. In addition, a subdivision was made of the type 2 spikes on the basis of their appearance on the rate plots. Some of the spikes show a very sharp boundary on the poleward side, and these are designated as type 2A. Spikes of this type were observed only at the trapping boundary. Examples of each type are shown in Figure 3. Unless specified otherwise, references to type 2 spikes do not include type 2A.

The location of a spike relative to the trapping boundary was determined from the D3 rate, since this had a finer resolution, and thus usually showed the most detail. The boundary was defined as that point where the D3 rate reached the polar plateau level, if there was no spike obscuring that point. If a spike was overlapping the point where the boundary seemed to be, that spike was designated type 2. Since this method requires visual inspection and some subjective decision, there is some ambiguity in several cases, and it is possible that a few of the spikes have been assigned to the wrong population. This has not caused any obvious difficulties, but it should be remembered when examining the results, especially near local midnight, where there is considerable overlap.

McCoy [1969] has observed that while most spikes do not recur on successive passes, in some cases a spike may be observed twice at a pair of nearly conjugate points, and in a few rare cases the "same" spike may be present and detectable for several hours. We confirm this observation. In fact, on two occasions we observe what appear to be related series of events lasting over eleven hours, and we observe several groups of shorter duration. All of the larger groups occur between 2200 and 0100 MLT, and within one degree of the outer zone boundary. Some of the smaller groups,

with observable lifetimes of about two hours, occur nearer the dawn-dusk meridian. The development of one of the large groups is illustrated in Figure 4. This behavior would seem to indicate that the time scales associated with spikes are of the order of minutes to several hours, and that the rapid rise and fall characteristic of a spike observed during a given pass represents a purely spatial effect. Parameters associated with these observations are listed in Table 2. The Λ values listed in this table have a standard deviation of nearly one degree, which indicates about the limit of accuracy of the values used throughout this paper. Errors of this magnitude arise from the field model [Jensen and Cain, 1962] used to calculate L, and the 6-10 second resolution (about 0.3 - 0.6 degrees) associated with reading spike times from data plots.

Data

We examined all the data available from rev 24 (30 July 1967) to rev 2293 (31 December 1967). During this period the experiment was turned on about 50% of the time. Due to the location of ground stations, we lack (tape-recorded) playback data for many passes at latitudes where spikes usually occur. This leaves us with approximately 2400 passes (maximum of four passes per orbit) through the "spike region," i.e. Invariant Latitudes $60° \leq \Lambda \leq 78°$, for which we have useful data. All local times have been sampled without any obvious bias, and so it is tempting to assume that the data represent uniform coverage of all local times. We will do this for the moment, but a detailed discussion of the coverage problem will be presented in a later section.

The data to be presented here represent 774 spike observations, of which about 50 to 100 probably are multiple observations of a smaller

number of long-lasting events. Figure 5 shows all of the spikes plotted in Invariant Latitude (Λ) versus Magnetic Local Time (MLT) coordinates. (Invariant Latitude is defined as $\cos \Lambda = \sqrt{1/L}$, with L calculated from the Jensen and Cain 1960 [Jensen and Cain, 1962] field. See Fritz and Gurnett [1965] for a definition of MLT, but note that the vector products in the denominator of their equation should be cross products.) Notice the significant local time asymmetry: there are comparatively few events between 0600 and 1200, while there is a large maximum between 2200 and 0400. Notice also that there are very few events which seem to be on open field lines, and that the events cluster about the trapping limit.

Figure 6 shows the same data mapped along field lines into the equatorial plane. The mapping used is that of Fairfield [1968]. Included for later discussion are regions where other investigators have observed spikes.

The first step in analyzing the data was to take a detailed look at the Λ - MLT dependence for each population. In doing this it was found that, while some very interesting patterns emerged, there was still a large amount of scatter in the data. It was thought that some of the variation in latitude at a given local time might be related to geomagnetic activity. To check this assumption, spikes of each type were grouped into local time bins such that the variation of Λ with MLT within each bin was no larger than the scatter in Λ. Plots were then made of Λ versus Kp for the spikes in each bin, and it became apparent that a significant effect was indeed present. One such plot is shown in Figure 7. Since the data were broken down into so many bins, statistics became poor, and justified nothing more than a straight-line fit to the Λ - Kp dependence in each bin. A linear regression analysis was performed on the data in each bin, and the

results are shown in Table 3. Using these results with some smoothing, it is possible to define a new latitude Λ', which is the latitude of occurrence of a spike corrected to Kp = 0. This reduced the scatter at a fixed MLT, but only by about 10% to 30%.

Plots of Λ' versus MLT are shown in Figure 8. Several observations may be made about these plots. First, it seems reasonable to assume that the strong dependence of Λ' on MLT for type 3 spikes is due to the distortion of the outer magnetosphere. Second, it can be seen that the high rate of occurrence of spikes near local midnight is due primarily to type 2 spikes, especially those of type 2A. Notice the pronounced clustering of the latter near local midnight.

In an attempt to determine whether the remaining scatter in Λ' could be attributed to any systematic effect, the local time variations, represented by Fourier series fits to the data in Figure 8, were subtracted out. The resulting quantity was plotted against Universal Time and against the angle between the earth's dipole axis and the earth-sun line. No dependence was found in either case. This leads us to suspect that the remaining scatter is due to 1) inaccuracy in the model of the internal field [Jensen and Cain, 1962] used to generate the original Λ values, 2) mislabelling of some of the spikes, 3) errors of a few seconds in reading times from data plots, 4) neglect of the external field in calculating Λ, or 5) true spatial fluctuations in the process that produces the spikes. Since this remaining scatter is large compared to the reduction in scatter achieved by extrapolating to zero Kp, the remainder of the discussion will not include this correction.

The distributions of the intensities and spectral hardnesses of the spikes are of interest for comparison with possible production mechanisms.

The peak counting rates $D1\overline{D3}$ and $D2\overline{D3}$, corrected for background, have been determined for each spike. Due to the 15-second averaging, these will be underestimates of the true peak values for narrow spikes, but will be good estimates for the average flux. We find that the type 2A spikes seem to be much harder spectrally than the others. The type 3 spikes may be slightly softer on the average than either the type 1 or type 2 spikes.

It is not surprising to find that larger events tend to occur during magnetically disturbed periods. There is a slight correlation between the $D1\overline{D3}$ rate and Kp value, but plots of $D1\overline{D3}/D2\overline{D3}$ against Kp indicate no significant dependence, except for a slight positive correlation probably due to the pileup effect in the $D1\overline{D3}$ rate.

Finally, Figure 9 shows the number distribution of spike intensities. The levelling-off at small values of $D1\overline{D3}$ is probably due in part to the difficulty of detecting small spikes and should not be considered significant.

Magnetic Local Time and Kp Dependence

In order to obtain the correct dependence of spike occurrence on such parameters as MLT and Kp, it is necessary to correct the observations for non-uniform sampling. It is common practice, when treating data of this kind from a polar orbiter, to make a cursory check to see that all local times have been sampled more or less uniformly, and then to assume that the coverage is indeed uniform and random. This procedure may conceal some peculiarity in the orbit, or accidental correlations between orbit parameters and telemetry coverage.

To investigate these possibilities and to correct for them, we employed the following procedure (similar to that used by Fritz and Gurnett [1965]). Data plots were examined to determine times for which useable data were available and processed, regardless of whether or not spikes were present. Then, spacecraft attitude/orbit data for these times only, and for $\Lambda > 55°$, were selected for further processing. The orbit sections thus selected were examined in detail, and their distributions in Λ-MLT-Kp space were computed, summarized, and used to normalize the spike occurrences.

Figure 10 shows the distribution in MLT of the occurrences of spikes of various types. The comparison between the raw number of occurrences and the normalized data gives some indication of the importance of the normalization. For instance, it indicates that the apparent local maximum in the occurrence of type 3 spikes near 0500 MLT is an effect of non-uniform coverage. This, combined with the possibility of a few misidentified spikes at other local times, indicates that the local-time dependence of type 3 spikes is not significantly different from a uniform distribution in the dawn hemisphere. The peak near 1300 MLT may be related to the position of the neutral point, as will be discussed below. The overall local-time behavior is similar to that obtained by Fritz and Gurnett [1965] for electrons with $E_e \geq 10$ kev. The absolute numbers are not directly comparable, however, due to the difference in energy thresholds and the difference in the threshold intensity for a spike to be counted. A rough comparison, neglecting the difference in solar activity, can be made if we assume an $E^{-3.5}$ differential energy spectrum to map their flux threshold for $E_e \geq 10$ kev ($j \geq 2.5 \times 10^7$ electrons $cm^{-2}sec^{-1}ster^{-1}$) to our energy threshold. The corresponding flux for $E_e \geq 425$ kev would be approximately

2.1×10^3 electrons $cm^{-2}sec^{-1}ster^{-1}$, and the corresponding $D1\overline{D3}$ counting rate is about 140 sec^{-1}. About 15% of our spikes (average of all types) are larger than this (cf. Figure 9), so we should multiply the normalized occurrence scale in Figure 10 by 0.15 to make the comparison. This gives about a 5% peak occurrence probability near local midnight, which compares well with the value of $\sim$ 4% reported by those authors. We also get qualitative agreement with their latitude and Kp dependences. Although the absolute numbers depend strongly on the assumed spectrum, this procedure shows that it is not unreasonable to assume that the spikes we observe at energies above 425 kev are simply manifestations of the high-energy tails of large events observed at much lower energies.

The normalized dependence of spike occurrence on Kp is shown in Figure 11. Here the correction for non-uniform sampling is even more important, since there are very few passes at high Kp. As might be expected, spikes are observed more frequently at times of high Kp, except those of type 2A, which appear to show the opposite behavior.

Discussion

The most striking feature of the data presented here is that the spikes can be grouped into several distinct populations with widely different characteristics. This grouping emphasizes the organizing power of various physical parameters, allowing more reliable and accurate descriptions of the phenomena and possible source mechanisms. We assume that there are only three possible sources for spikes observed at low altitudes: 1) local acceleration on lines of force connected to the region of observation, 2) scattering from the stably trapped population, and 3) transport from various regions of the outer magnetosphere,

possibly accompanied by acceleration. These will be discussed in relation to each spike type.

Type 1 spikes have several characteristics which point to their most likely source: 1) by definition, they occur at latitudes below the trapping limit, and so are on closed field lines and able to exhibit trapped or pseudo-trapped behavior; 2) they are not observed to persist on successive orbits, indicating lifetimes less than about 100 minutes; 3) their intensities are not much larger than that of outer zone trapped electrons. These observations are consistent with local acceleration or pitch angle scattering from the stably trapped population into the loss cone. While we are not able to distinguish between these alternatives on the basis of the data presented here, the second possibility appears far more attractive. Strong pitch-angle scattering is fairly well understood [Kennel and Petschek, 1966], although the details for impulsive events at the energies we observe have not been discussed explicitly. It is unlikely that the trapped 425 kev electron flux is near the point of self-excitation of the Kennel and Petschek mechanism, but scattering at this energy might be caused by interactions with waves generated by lower energy particles. Local acceleration to relativistic energies would seem less likely.

Type 3 spikes present a totally different picture. Their latitude-local time dependence strongly suggests that they are occurring near the "last" closed field line at every local time. This means that they occur on lines which approach the magnetopause or the neutral sheet, depending on the local time at the foot. The peak in occurrence just east of local noon (see Figure 10) indicates possible connection to the neutral point, where field turbulence might be expected to be large. Several experimenters (see Figure 6) have observed similar impulsive fluxes of high energy electrons

both near the magnetopause and near the neutral sheet, and Meng and Anderson [1970] have observed a sheet of electrons (> 40 kev) near the magnetopause. The source mechanism(s) for these events has not been definitely established, but it seems likely that the low altitude spikes of type 3 and the distant fluxes may be manifestations of the same process. Notice, however, that the mapping of Fairfield [1968] (Figure 6) indicates that the precipitating spikes are associated not with the magnetopause, but with the flanks of the magnetosphere. Both a better field model and simultaneous observations at low altitudes and near the magnetopause are needed to distinguish between these possibilities.

The type 2 spikes (and especially type 2A) present an even more interesting picture. The strong day-night asymmetry and the latitude of occurrence near midnight ($\Lambda \simeq 67°$) indicate that these events are related to the neutral sheet and/or the cusp region. Hones et al. [1971] have observed an energetic electron spike simultaneously at 1, 6.6, and 18 earth radii near local midnight. This confirms the interpretation that neutral sheet spikes and low altitude spikes are directly related. A likely acceleration mechanism would be merging of field lines in the neutral sheet and subsequent collapse of the stretched field lines into a dipole-like configuration, perhaps preceded by particle precipitation and field deflation at $L \simeq 4$-6. This process has been suggested by Axford [1969], and observed by McPherron and Coleman [1970], and by Lezniak and Winckler [1970]. The results of Arnoldy and Chan [1969] seem to indicate that electron spikes observed at 6.6 R_E have drifted from an injection point at local midnight. Moreover, the observations of Hones et al. [1968] indicate that the source is probably nearer than 17 R_E to the earth. Parks [1970], however, has attributed some events of this type to strong pitch angle diffusion.

The type 2A spikes are of special interest, since their characteristically sharp cutoff on the high-latitude side and their strong tendency to occur conjugately indicate that they may define very accurately the last closed field line near local midnight. Examination of Figure 4 illustrates this clearly. The spike first appeared at 1910 UT during the north polar pass of rev 827. At this time the trapping limit was at a higher latitude, but within 50-60 minutes it had moved down to the latitude of the spike. The configuration of the magnetosphere then apparently remained fairly stable for about ten hours, until some time between 0500 UT and 0720 UT, when the spike disappeared rather abruptly. This should not be assumed to be a common occurrence, however, since only two events of such long duration were observed, and since the scarcity of type 2 events on the day side and the short lifetimes of type 1 and type 3 spikes indicate that stable trapping of spike particles is uncommon. The results of Arnoldy and Chan [1969] indicate that the decay time at 6.6 R_E is probably about the same as the drift period for electron energies 50 kev $\leq E_e \leq$ 150 kev.

Summary

The vertical particle telescope on OGO 4 has detected numerous spikes of precipitating electrons with energies above 425 kev. These occur within a few degrees of the high-latitude boundary of the outer zone, and have characteristic widths on the order of one degree in latitude. The time scale for buildup and decay of an event is of the order of several minutes to several hours.

It is instructive to group the spikes into several populations on the basis of their latitude with respect to the outer zone boundary. The local-time dependence is highly non-uniform, with at least five times as many events occurring near 2200 MLT as near 1000 MLT. The disparity is much greater (about 12:1) if only those spikes occurring at or below the outer zone boundary are considered.

The average Invariant Latitude of occurrence is 67°-68°, but this is strongly dominated by the large number of spikes occurring near local midnight. They tend to occur at higher latitudes, and to have a larger spread in latitudes, near local noon. The effect of local time on latitude is strongest for those spikes which occur above the trapping boundary.

Latitude of occurrence is also affected by geomagnetic disturbance, as indicated by the Kp index. The latitude tends to be decreased by about 0.6 ± 0.3 degrees per unit Kp, and this effect is stronger near local noon than near midnight.

Fits to assumed power-law spectra indicate an average spectral index of 4 to 5 (or e-folding energies of 130 to 170 kev for exponential spectra), except for special large, characteristically-shaped events (type 2A) which occur at the trapping boundary near local midnight and have a spectral index around 3 for power-law (or 260 kev e-folding energy for exponential). The median flux (E_e > 425 kev) is about 150 electrons $cm^{-2}sec^{-1}ster^{-1}$, except for the low-latitude (type 1) events and the special (type 2A) events mentioned above, which are about five times as large.

Acknowledgements

We gratefully acknowledge the collaboration and support of Drs. J. A. Simpson and C. Y Fan during various stages of the joint University of Chicago/California Institute of Technology program. The instrument was constructed by the Laboratory of Astrophysics and Space Research of the University of Chicago. This work was performed under contract NAS5-3095 and grants NGL 05-002-007 and NGR 05-002-160. J. W. Brown received valuable support from the National Science Foundation.

TABLE 1. Detector response

Detector(s)	p	α	e*	$A\Omega_{p,\alpha}$	$A\Omega_e$(max.)
	(Mev)	(Mev)	(Mev)	(cm^2ster)	(cm^2ster)
$D1\overline{D3}$	1.22-39.2	4.88-157	0.45-1.8	1.05-1.18	0.08
$D2\overline{D3}$	9.32-39.2	37.3-157	0.7 -4	1.50-1.56	0.36
$D1D2\overline{D3}$	9.32-39.2	37.3-157	-	1.05-1.18	0
D3	$\gtrsim$ 9.3	$\gtrsim$ 37	$\gtrsim$ 0.5		

*Electron energies at which $A\Omega_e \gtrsim 0.5\ A\Omega_e$(max.)

TABLE 2. Parameters associated with the persistent spike shown in Figure 4.

REV	UT*	Λ	MLT	$D1\overline{D3}$ †	$D2\overline{D3}$ †
827N	1910.3	67.0	1.1	67	107
827S	1946.0	65.2	0.8	97	98
828N	2048.3	67.3	1.6	16	250
828S	2126.0	67.2	0.2	250	250
829N	2226.4	67.9	2.1	--- NO DATA	---
829S	2305.7	67.1	23.7	250	320
830N	0004.8	68.3	2.3	--- NO DATA	---
830S	0045.3	67.3	23.6	490	620
831N	0143.4	69.3	2.1	--- NO DATA	---
831S	0224.0	66.7	0.0	390	620
832N	0323.0	68.0	1.4	24	75
832S	0402.6	67.2	0.8	400	500
833N	0502.2	67.8	0.7	--- NO DATA	---
833S	------	-- NO	DATA --	---	---
834N	------	-- NO	DATA --	---	---
834S	0719.0	68.5	3.0	8	14

* Hours, minutes, tenths.

† Counting rates, counts/second.

TABLE 3. Results of regression analysis: linear fit of Λ versus Kp in various MLT intervals.

TYPE	MLT	NUMBER OF SPIKES	$\langle\Lambda\rangle$	SLOPE ($d\Lambda/dKp$)
1	0-4	44	65.0	+.03±.26
1	4-9	15	64.2	+.09±.27
1	9-16	22	66.8	-.48±.22
1	16-21	40	64.3	-.92±.27
1	21-24	38	65.3	-.97±.19
2	0-4	88	67.3	-.39±.12
2	4-8	31	68.6	-.83±.18
2	8-15	27	69.5	-.23±.23
2	15-19	59	67.8	-.81±.17
2	19-24	89	66.4	-.61±.12
2A	0-4	54	66.8	-.65±.14
2A	4-19	13	68.4	-.82±.42
2A	19-24	68	66.2	-.68±.15
3	0-4	30	68.1	-.11±.29
3	4-7	32	70.3	-.07±.29
3	7-9	16	73.4	-.62±.32
3	9-11	12	75.9	-.49±.37
3	11-13	14	74.0	-1.06±.43
3	13-17	57	70.6	-.90±.28
3	17-24	25	68.3	-.55±.33

REFERENCES

Anderson, H. R., P. D. Hudson, and J. E. McCoy, Observations of POGO ion chamber experiment in the outer radiation zone, J. Geophys. Res., 73, 6285, 1968.

Anderson, K. A., Energetic electron fluxes in the tail of the geomagnetic field, J. Geophys. Res., 70, 4741, 1965.

Anderson, K. A., H. K. Harris, and R. J. Paoli, Energetic electron fluxes in and beyond the earth's outer magnetosphere, J. Geophys. Res., 70, 1039, 1965.

Arnoldy, R. L., and K. W. Chan, Particle substorms observed at the geostationary orbit, J. Geophys. Res., 74, 5019, 1969.

Axford, W. I., Magnetospheric convection, Rev. Geophys., 7, 421, 1969.

Evans, L. C., J. L. Fanselow, and E. C. Stone, User's notes for experiments C-08 and D-08 rate plots, Internal Report No. 11, Caltech Space Radiation Laboratory, Pasadena, California, 1970.

Fairfield, D. H., Average magnetic field configuration of the outer magnetosphere, J. Geophys. Res., 73, 7329, 1968.

Fan, C. Y., G. Gloeckler, and J. A. Simpson, Acceleration of electrons near the earth's bow shock and beyond, J. Geophys. Res., 71, 1837, 1966.

Frank, L. A., On the local-time dependence of outer radiation zone electron ($E > 1.6$ Mev) intensities near the magnetic equator, J. Geophys. Res., 70, 4131, 1965.

Frank, L. A. and J. A. Van Allen, Measurements of energetic electrons in the vicinity of the sunward magnetospheric boundary with Explorer 14, J. Geophys. Res., 69, 4923, 1964.

Fritz, T. A., and D. A. Gurnett, Diurnal and latitudinal effects observed for 10-kev electrons at low satellite altitudes, J. Geophys. Res., 70, 2485, 1965.

Hoffman, R. A., Low-energy electron precipitation at high latitudes, J. Geophys. Res., 74, 2425, 1969.

Hoffman, R. A., and D. S. Evans, Field-aligned electron bursts at high latitudes observed by OGO-4, J. Geophys. Res., 73, 6201, 1968.

Hones, E. W., Jr., R. H. Karas, L. J. Lanzerotti, and S. I. Akasofu, Magnetospheric substorms on September 14, 1968, J. Geophys. Res., 76, 6765, 1971.

Hones, E. W., Jr., S. Singer, and C. S. R. Rao, Simultaneous observations of electrons (E > 45 kev) at 2000-kilometer altitude and at 100,000 kilometers in the magnetotail, J. Geophys. Res., 73, 7339, 1968.

Jensen, D. C., and J. C. Cain, An interim geomagnetic field (abstract), J. Geophys. Res., 67, 3568, 1962.

Kennel, C. F., and H. E. Petschek, Limit on stably trapped particle fluxes, J. Geophys. Res., 71, 1, 1966.

Lezniak, T. W., and J. R. Winckler, Experimental study of magnetospheric motions and the acceleration of energetic electrons during substorms, J. Geophys. Res., 75, 7075, 1970.

Lupton, J. E. and E. C. Stone, Electron scattering effects in typical cosmic ray telescopes, IEEE Trans. on Nuc. Sci., NS-19, 562, 1972.

McCoy, J. E., High-latitude ionization spikes observed by the POGO ion chamber experiment, J. Geophys. Res., 74, 2309, 1969.

McDiarmid, I. B., and J. R. Burrows, Electron fluxes at 1000 kilometers associated with the tail of the magnetosphere, J. Geophys. Res., 70, 3031, 1965.

McDiarmid, I. B., and J. R. Burrows, Local time asymmetries in the high-latitude boundary of the outer radiation zone for the different electron energies, Can. J. Phys., 46, 49, 1968.

McPherron, R. L., and P. J. Coleman, Inward collapse of the magnetic tail during magnetospheric substorms (abstract), Trans. Am. Geophys. Union, 51, 402, 1970.

Meng, C. I., and K. A. Anderson, A layer of energetic electrons (>40 kev) near the magnetopause, J. Geophys. Res., 75, 1827, 1970.

Montgomery, M. D., S. Singer, J. P. Conner, and E. E. Stogsdill, Spatial distribution, energy spectra, and time variations of energetic electrons (E > 50 kev) at 17.7 earth radii, Phys. Rev. Letters, 14, 209, 1965.

Murayama, T., and J. A. Simpson, Electrons within the neutral sheet of the magnetospheric tail, J. Geophys. Res., 73, 891, 1968.

Parks, G. K., The acceleration and precipitation of Van Allen outer zone energetic electrons, J. Geophys. Res., 75, 3802, 1970.

Retzler, J., and J. A. Simpson, Relativistic electrons confined within the neutral sheet of the geomagnetic tail, J. Geophys. Res., 74, 2149, 1969.

Rosen, A., The radiation belt boundary near solar cycle maximum as determined from the trapping of energetic electrons, J. Geophys. Res., 70, 4793, 1965.

FIGURE CAPTIONS

Figure 1. OGO 4 vertical telescope cross section. Not shown is a magnesium wall which covers the inner side of the scintillator.

Figure 2. Real-time data from revolutions 2878 and 2880, showing large spikes. D1 data includes only those events which pulse-height analysis shows to be electrons. The events shown occurred at 0120 and 0125 MLT and had widths (FWHM) of 6 and 10 seconds. Neither of these events is included in the rest of the data presented.

Figure 3. Examples of data plots showing spikes of each type. Notice that the $D1D2\overline{D3}$ rate is much smaller than the $D2\overline{D3}$ rate for each spike, indicating electrons.

Figure 4. Development of a long-lasting event. The arrows indicate the position of the spike. Data for revolutions 826 and 835 show no spike, so we assume that this represents the complete history of the event. The sharp cutoff on the poleward side from revolution 828 to 833 is characteristic of type 2A spikes. Notice the more gradual blending into the polar rate in revolution 827 and 834. Invariant Latitude is indicated for revolution 827 only. See Table 2 for details of each spike.

Figure 5. Latitude-local time plot of all spike observations. Notice the relative scarcity of events between 0600 and 1200 MLT, and the clustering of events near the average trapping boundary. Boundaries are those of McDiarmid and Burrows [1968], determined from 35 kev electron data.

Figure 6. Data from Figure 5 mapped along field lines into the magnetic equatorial plane using the results of Fairfield [1968]. Points with tick marks attached were outside the range of the mapping, and probably should be moved in the direction indicated by the ticks. Regions where other experimenters have observed "island fluxes" of electrons far from the earth are included for comparison. Tick marks on axis lines are at $\pm$ 10 R_E. Local time orientation is the same as in Figure 5.

Figure 7. Sample plot of Λ versus Kp for a limited range of MLT, showing the tendency for spikes to occur at lower latitudes during magnetically disturbed times. The straight line is a least-squares fit to the points shown. The horizontal bars define the points included in the means. The vertical bars denote the standard deviations of the means.

Figure 8. Plots of "corrected" Invariant Latitude (Λ corrected to Kp = 0) versus Magnetic Local Time. Error bars have the same meaning as in Figure 7.

Figure 9. Relative number of spikes larger than a given value of $D1\overline{D3}$.

Figure 10. Number of spikes of each type as a function of MLT. Note that local midnight is in the center of the time axes, primarily to emphasize the Type 2A distribution. Also included are data normalized for unequal local-time coverage (see section on coverage normalization). Dotted lines represent raw counts, solid lines are normalized. Error bars refer only to the statistics associated with the number of events observed.

Figure 11. Relation between spike occurrence and Kp.

OGO-IV VERTICAL PARTICLE TELESCOPE

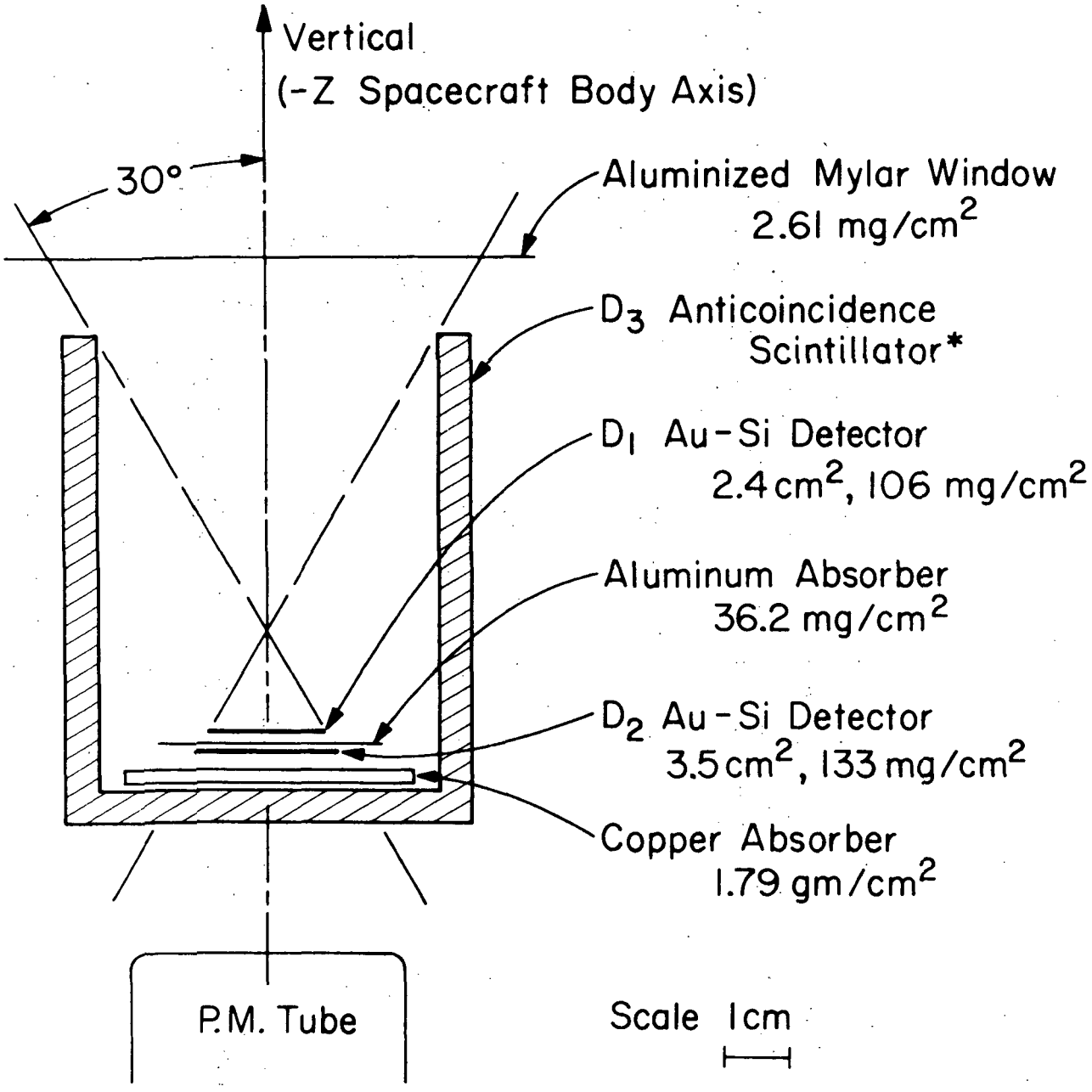

* Scintillator is surrounded by 138 mg/cm² of magnesium.

D_1 and D_2 both have depletion depths of 56 mg/cm².

Fig. 1

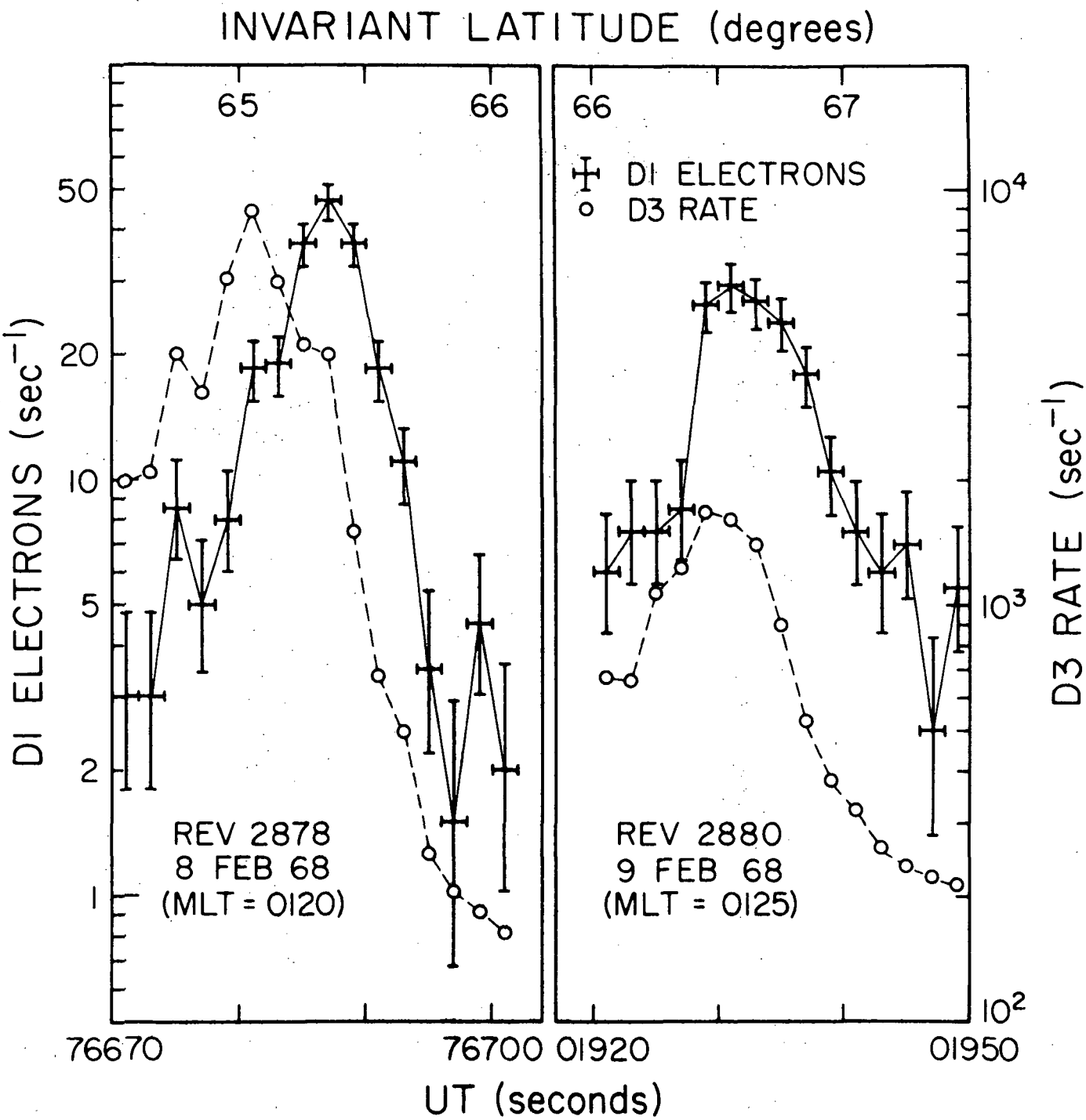
INVARIANT LATITUDE (degrees)
65
66
66
67
DI ELECTRONS
D3 RATE
50
20
10
5
2
1
10^4
10^3
10^2
DI ELECTRONS (sec^{-1})
D3 RATE (sec^{-1})
REV 2878
8 FEB 68
(MLT = 0120)
REV 2880
9 FEB 68
(MLT = 0125)
76670
76700
01920
01950
UT (seconds)

Fig. 2

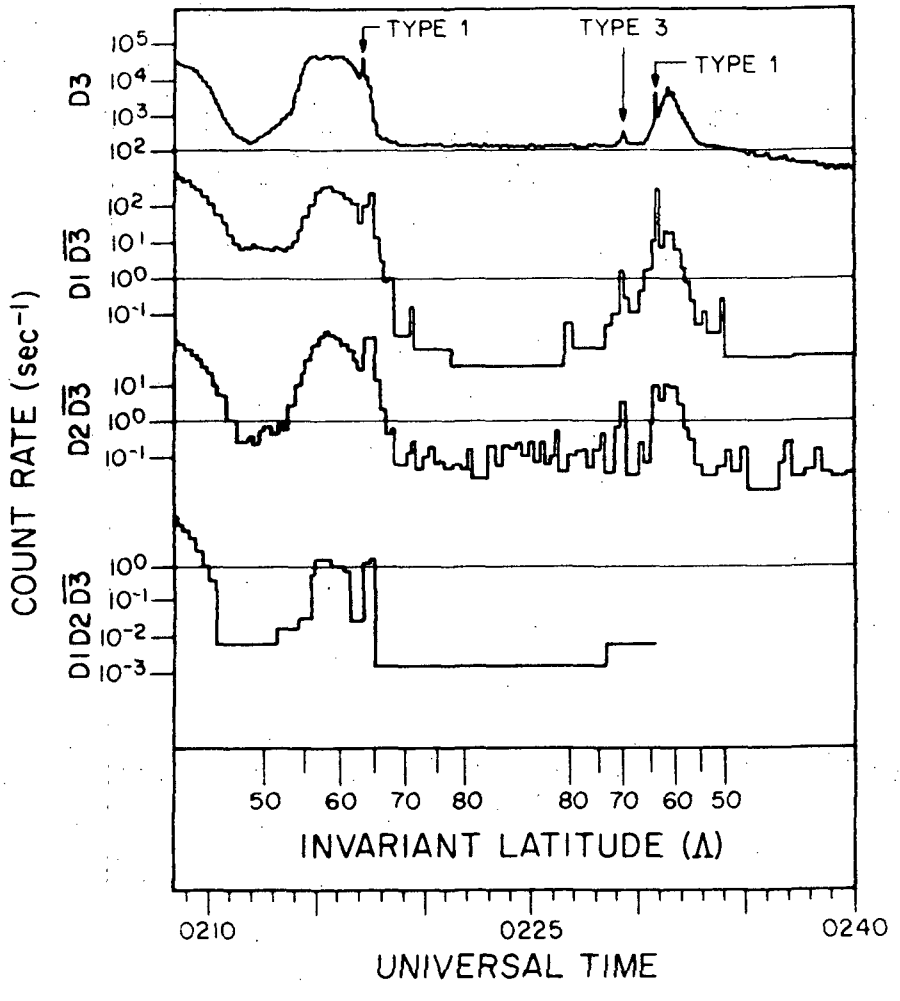

OGO-4 REV. 934 DAY 273 9/30/67
SOUTH POLAR PASS

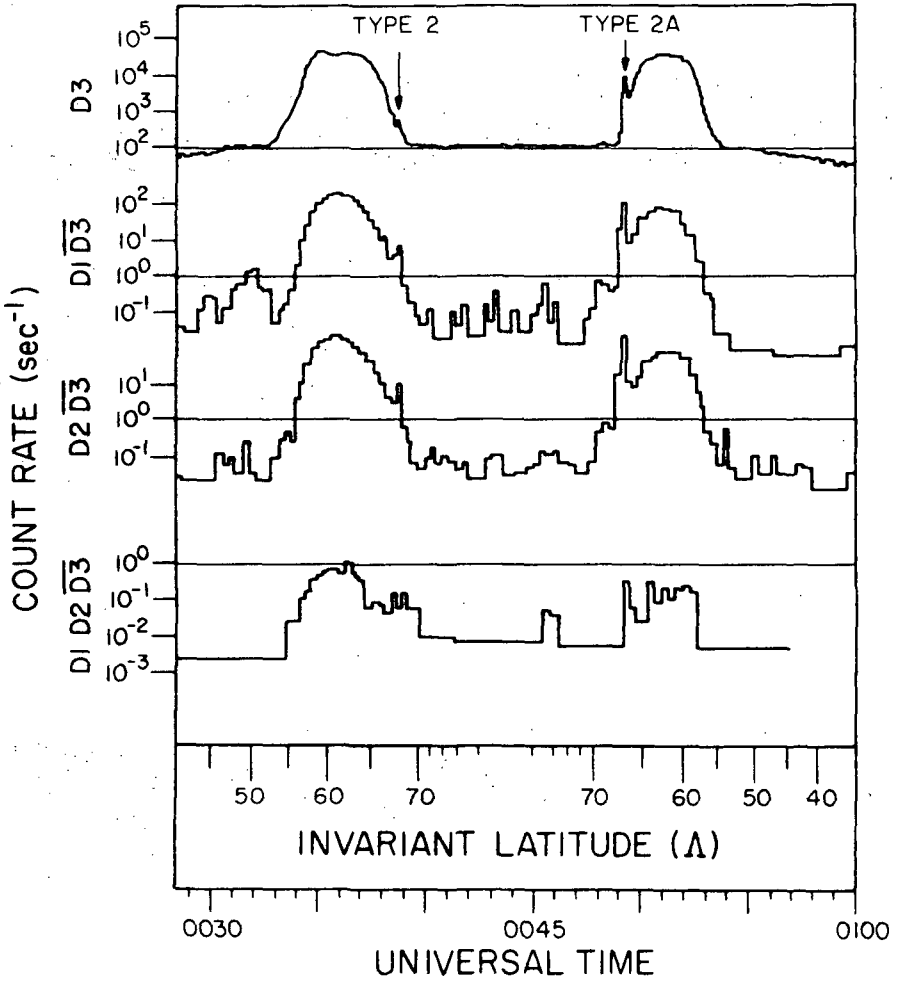

OGO-4 REV. 1979 DAY 344 12/10/67
SOUTH POLAR PASS

Fig. 3

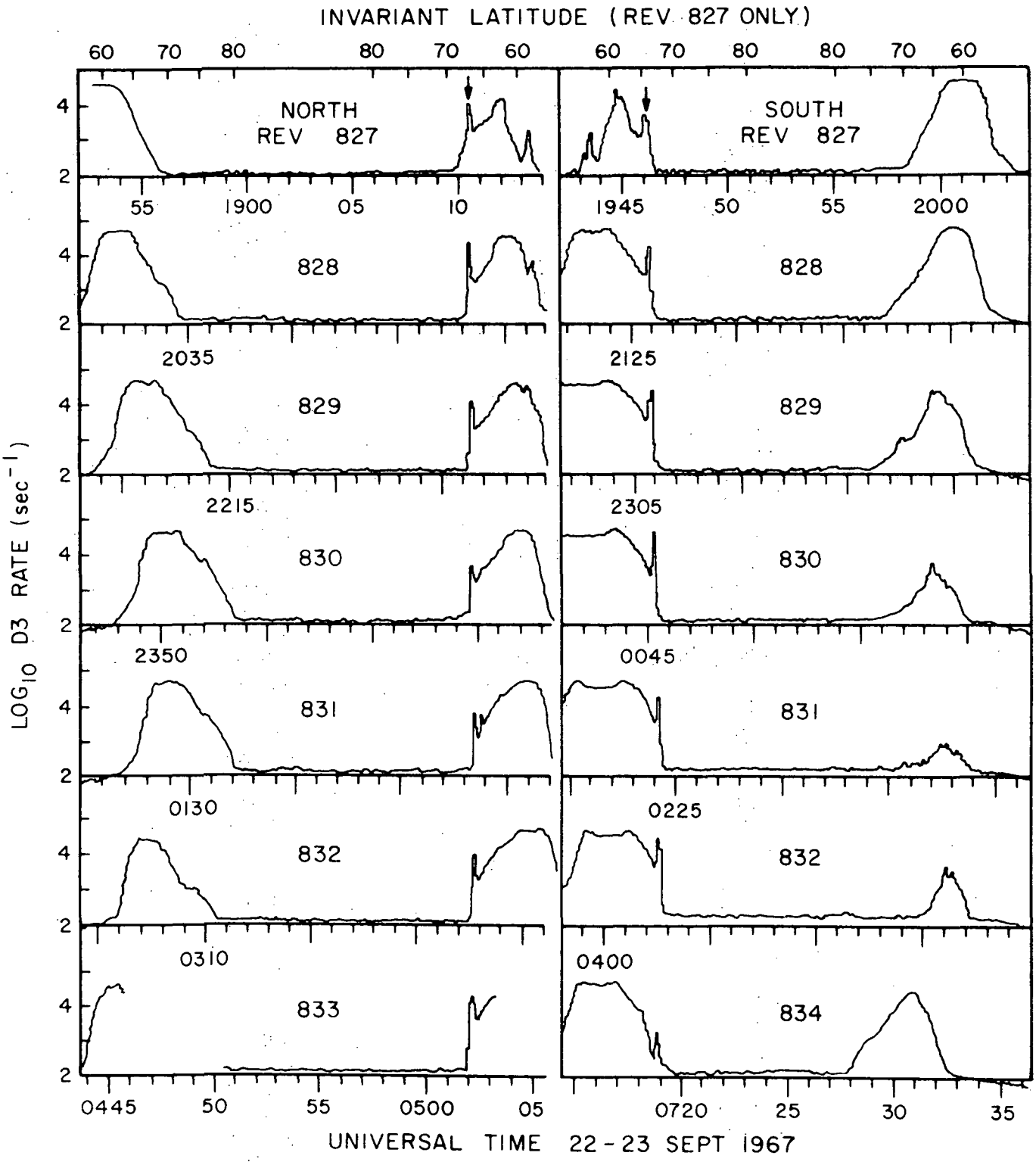
INVARIANT LATITUDE (REV 827 ONLY)
60 70 80 80 70 60
60 70 80 80 70 60
NORTH
REV 827
SOUTH
REV 827
55 1900 05 10
1945 50 55 2000
828
828
2035
829
2125
829
2215
830
2305
830
2350
831
0045
831
0130
832
0225
832
0310
833
0400
834
0445 50 55 0500 05
0720 25 30 35
UNIVERSAL TIME 22-23 SEPT 1967
LOG10 D3 RATE (sec-1)
4
2

Fig. 4

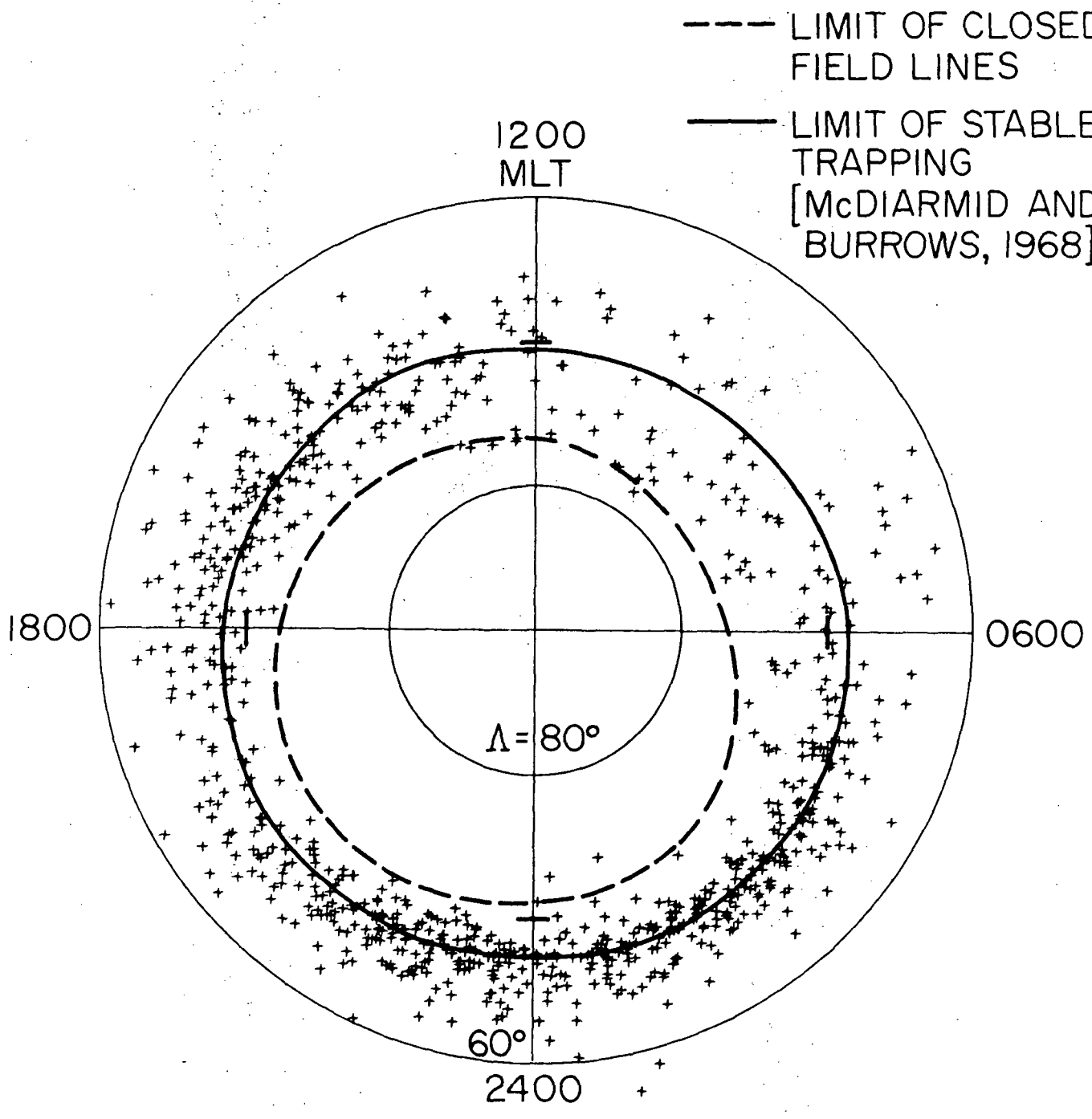
LIMIT OF CLOSED FIELD LINES
LIMIT OF STABLE TRAPPING [McDIARMID AND BURROWS, 1968]
1200 MLT
1800
0600
2400
Λ = 80°
60°

Fig. 5

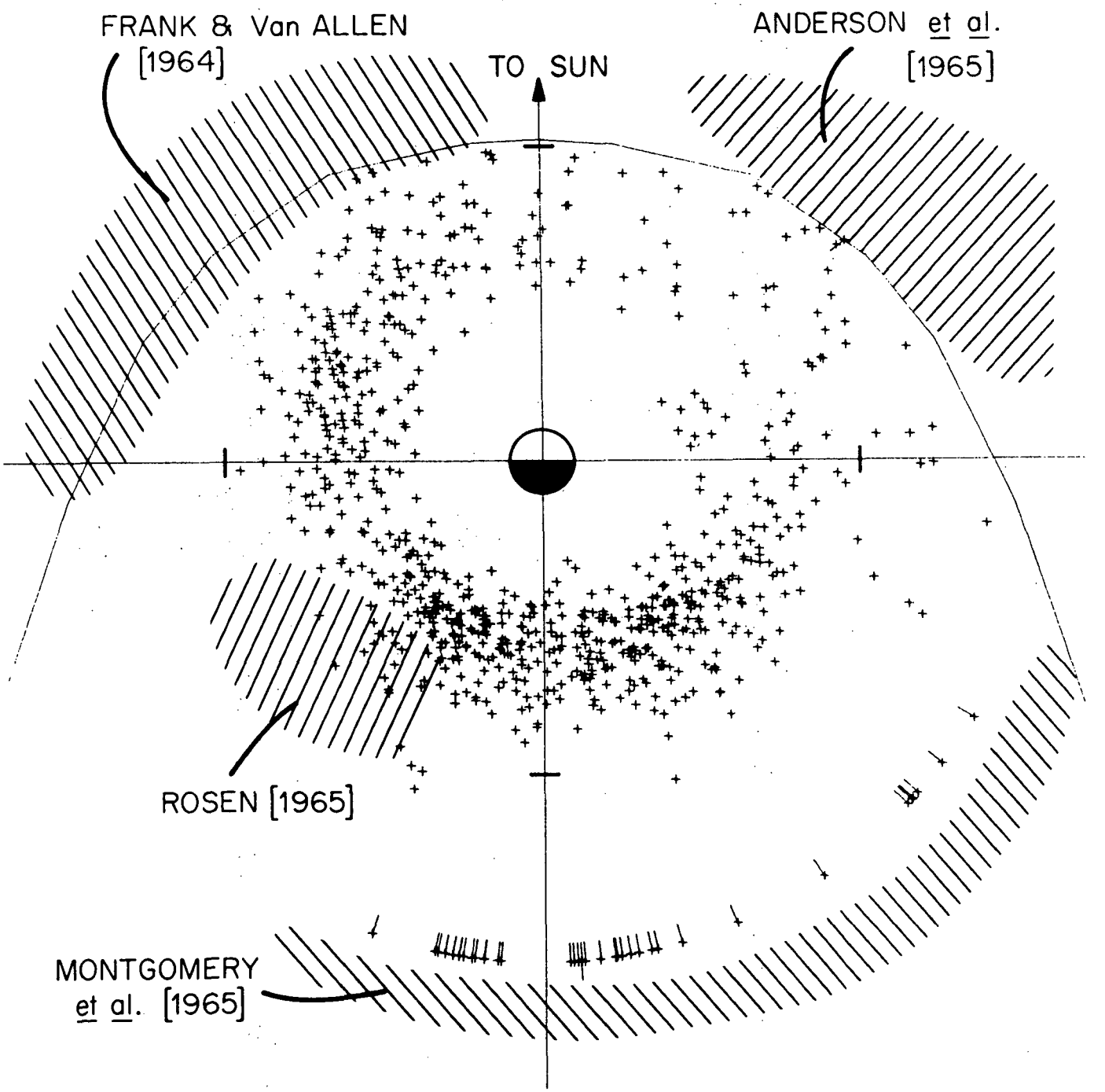
FRANK & Van ALLEN
[1964]
TO SUN
ANDERSON et al.
[1965]
ROSEN [1965]
MONTGOMERY
et al. [1965]

Fig. 6

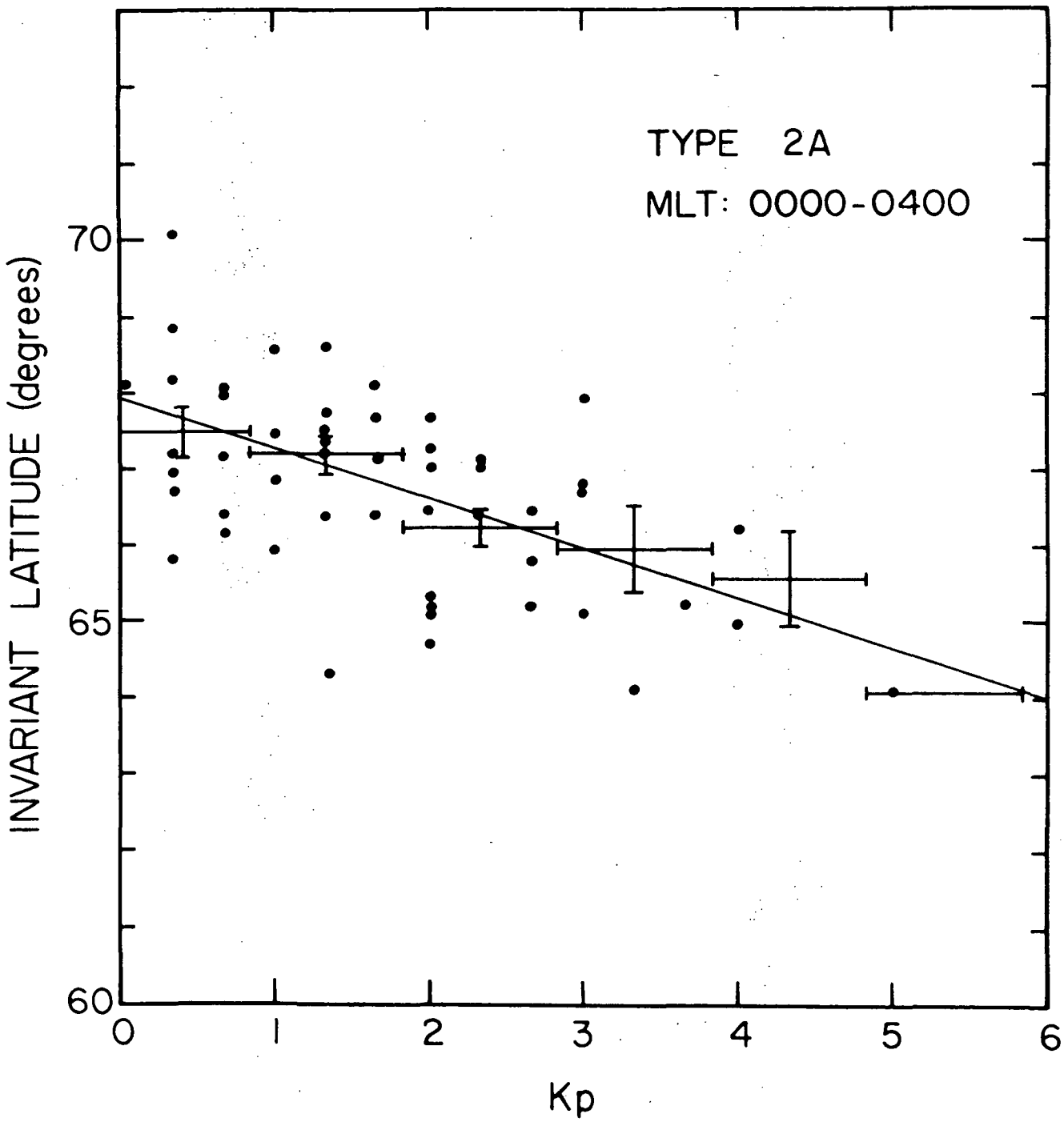
TYPE 2A
MLT: 0000-0400
INVARIANT LATITUDE (degrees)
70
65
60
0
1
2
3
4
5
6
Kp

Fig. 7

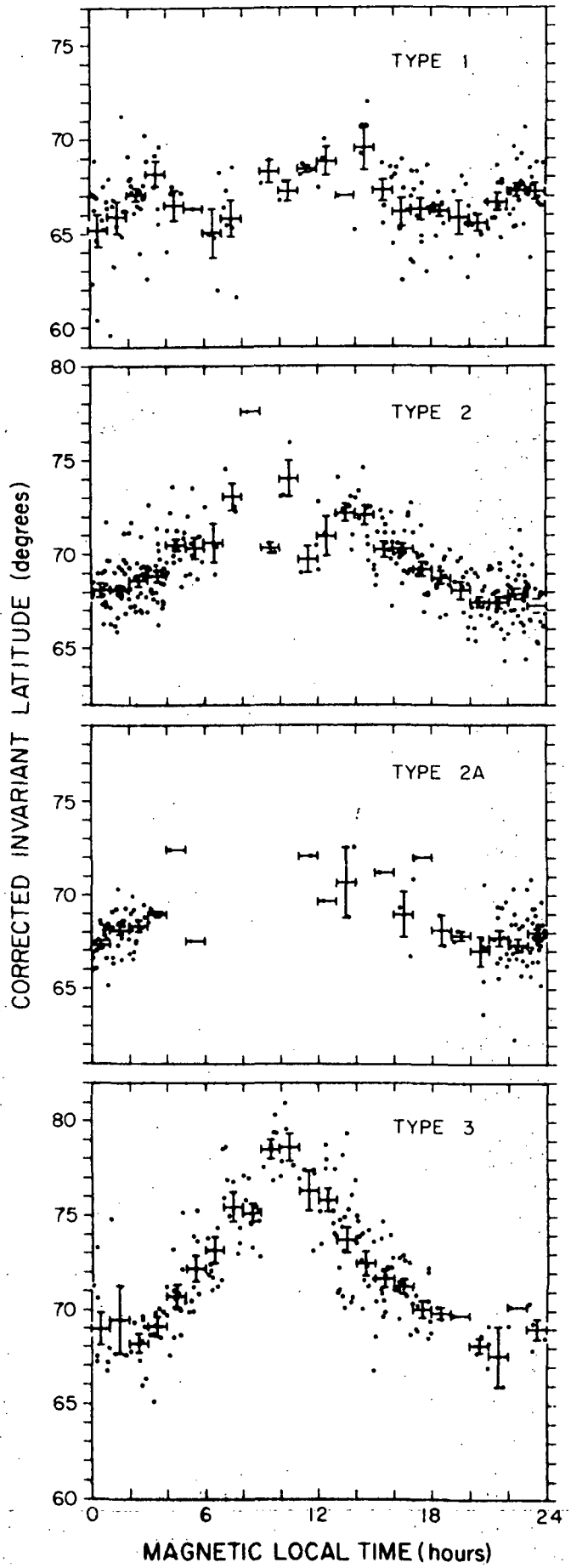
TYPE 1
TYPE 2
TYPE 2A
TYPE 3
CORRECTED INVARIANT LATITUDE (degrees)
MAGNETIC LOCAL TIME (hours)
75
70
65
60
80
0
6
12
18
24

Fig. 8

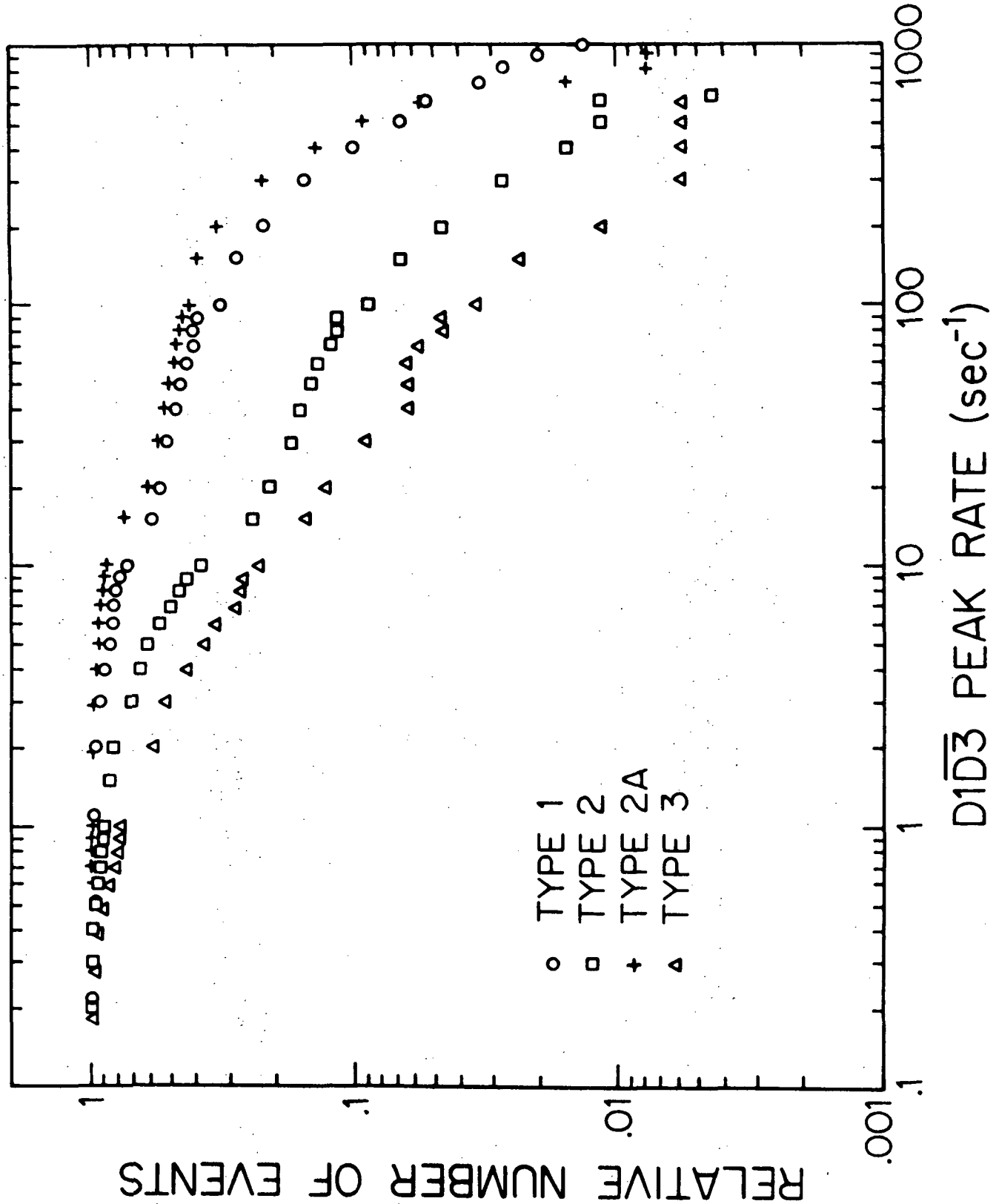
RELATIVE NUMBER OF EVENTS
1
.1
.01
.001
.1
1
10
100
1000
D1$\overline{D3}$ PEAK RATE (sec^{-1})
TYPE 1
TYPE 2
TYPE 2A
TYPE 3

Fig. 9

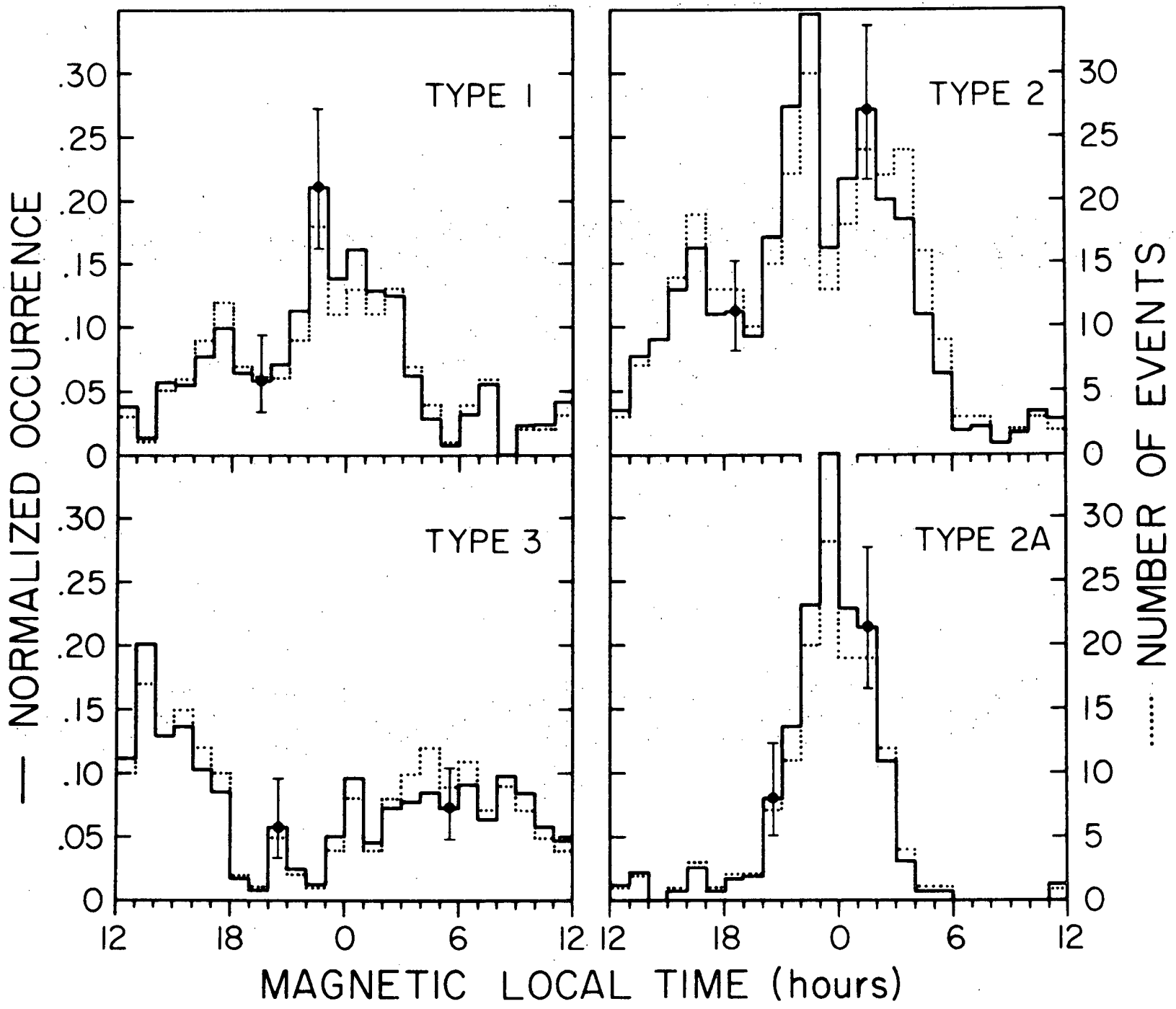
TYPE 1
TYPE 2
TYPE 3
TYPE 2A
— NORMALIZED OCCURRENCE
..... NUMBER OF EVENTS
.30
.25
.20
.15
.10
.05
0
30
25
20
15
10
5
0
12
18
0
6
12
MAGNETIC LOCAL TIME (hours)

Fig. 10

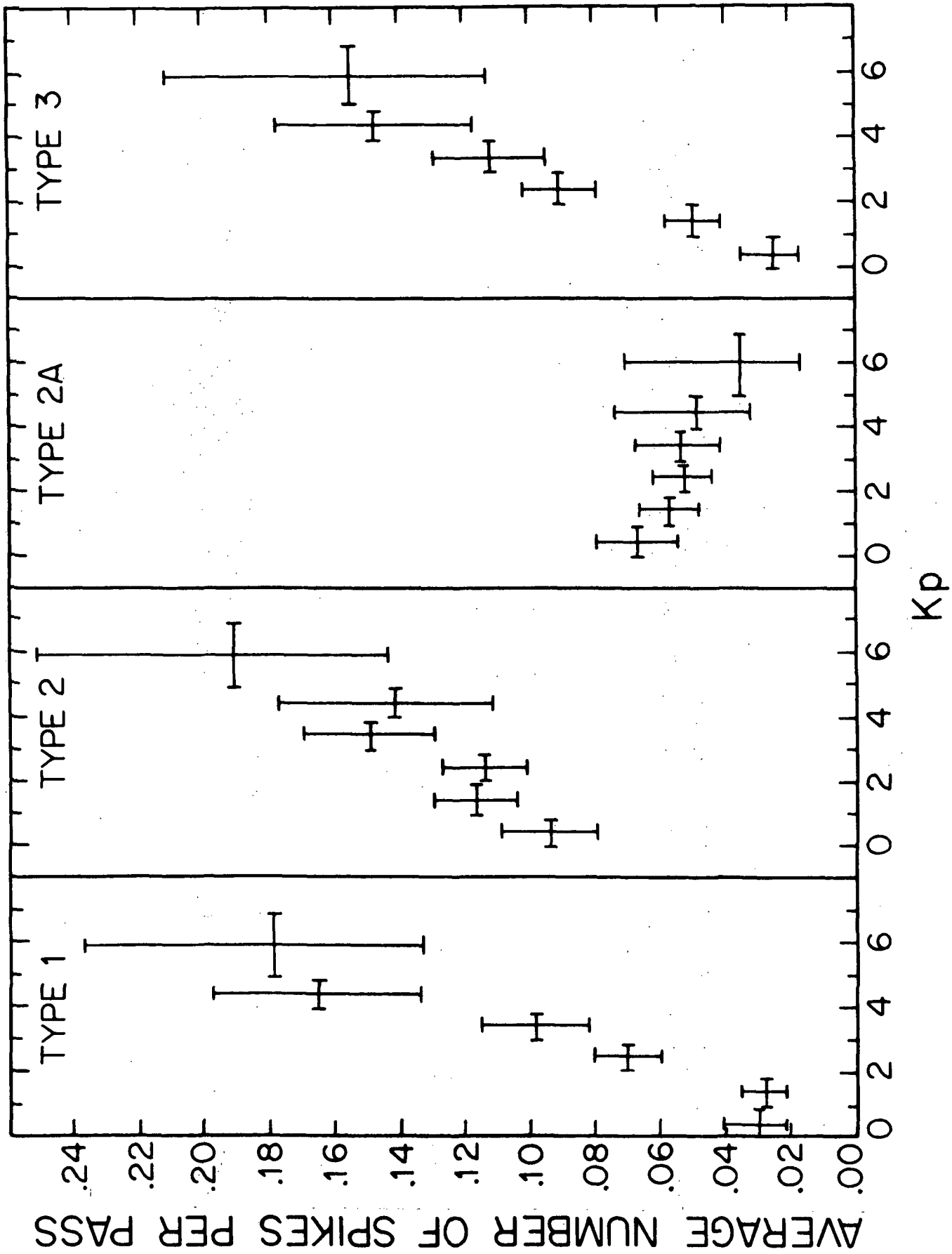
AVERAGE NUMBER OF SPIKES PER PASS
.24
.22
.20
.18
.16
.14
.12
.10
.08
.06
.04
.02
.00
TYPE 1
TYPE 2
TYPE 2A
TYPE 3
0 2 4 6
Kp

Fig. 11